A high-precision X-ray beam-position and profile monitor for synchrotron beamlines

R. G. van Silfhout

EMBL, c/o DESY, Notkestrasse 85, D-22603 Hamburg, Germany.
E-mail: silfhout@embl-hamburg.de

A novel monitor for X-ray beam position, intensity and profile is presented. This diagnostic instrument is based on a commercial photodiode array which detects X-rays scattered diffusely from a featureless foil. The typical accuracy with which the beam position is determined is 1 µm. Although initially conceived for the characterization of 'white' synchrotron radiation, this monitor has proven to be suitable for monochromatic radiation as well, hence providing a single solution to the task of beam characterization along the X-ray beam path, from source to sample.

1. Introduction

Recently, significant advances have been made in the design of optical components that preserve the high brightness of third-generation synchrotron radiation sources. State-of-the-art focusing optics and cryogenically cooled monochromators routinely produce intense highly collimated X-ray beams. The beam cross section has diminished to the extent that minute variations in beam position degrade the brightness of the source and severely impair experiments that study extremely small samples. Relative displacements among the individual optical components caused by varying power loading between synchrotron refills, source and floor movements are reduced by proper design but never removed completely. Hence, beamline designers are now confronted by a new challenge: preserving the brightness of the X-ray beam as measured at the sample position over time.

High-precision diagnostic instruments for beam position and intensity are indispensable devices in any procedure aimed at stabilizing the brightness of X-ray beams. In order to determine the brightness of the X-ray beam one must measure not only the beam intensity but also the photon flux density over the cross section of the beam. Most of the existing beam-position monitors, however, only measure beam position by intercepting parts of the beam with photoemission (Koyama *et al.*, 1989), photoelectric (van Silfhout, 1998) and calorimetric (Rosenbaum & Fornek, 1997) devices. The beam position as inferred from these devices will be incorrect when the beam profile changes. Beam-position monitors which are insensitive to the shape of the beam are based on two triangular-shaped foils (Johnson & Oversluizen, 1990). The ratio of the photo-emission signal produced by the X-ray beam on the two foils is very sensitive to the beam position. A disadvantage

of photoemission detectors is that the designer has to shield the electrodes carefully from photoelectrons originating from nearby sources such as slits. This usually involves adding extra foils into the beam path. With these earthed foils the device also serves as a very sensitive device for detection of vibrations, adding considerable noise to the measurements. Split ion chambers (Izumi *et al.*, 1989) are not compatible with the ultrahigh vacuum environment of a beamline.

The spatial distribution of the X-ray flux has been measured by observing the Bragg reflection of a thin beryllium crystal with a camera system (Fajardo & Ferrer, 1995). Unfortunately, the use of a crystal in the beam causes a strong variation in the extinction of the beam as a function of X-ray energy due to Bragg reflections of the beryllium crystal rendering the device unsuitable for spectroscopic measurements. Moreover, the accuracy of this device is rather low, of the order of 10 µm.

In this article we present a simple design for a low-cost X-ray beam monitor which measures the beam intensity and projected spatial flux distribution. The device has been tested with 'white' (or polychromatic) and monochromatic radiation with characteristics superior to existing monitors. The device has a high precision and a good long-term stability, it is ultrahigh-vacuum compatible and it can be placed in the beam path permanently. Our monitor is based on a linear photodiode array which detects the X-rays scattered out of the beam by a thin featureless foil. X-ray beam monitors based on measurements of the radiation scattered diffusely by a weakly absorbing foil have been used elsewhere as simple beam-intensity monitors on many X-ray beamlines, but the use of the diode array also allows us to measure the beam position and the beam profile simultaneously. Using this low-cost design it becomes feasible to have multiple beam monitors on a single

beamline. In this way the influence of the various optical components could be monitored and any loss of brightness detected quickly and precisely.

2. Design and implementation

In Fig. 1 a schematic of our beam monitor design is shown. A negligible amount of radiation is diffusely scattered out of the X-ray beam by a thin featureless foil. The type of foil chosen depends on the brightness of the beam. For intense polychromatic or 'white' radiation, for example, very thin ($\leq$10 µm) carbon (UCAR Inc., USA) or beryllium (Electrofusion Inc., USA) foils produce sufficient scattered radiation for acceptable signal levels. For monochromatic beams we resort to 10–50 µm-thick aluminium foils. The angle of incidence α (see Fig. 1) of the X-ray beam with the surface of the foil determines the size of the footprint of the beam on the foil. By using angles α lower than 45° a beam movement of size Δ will cause a movement of the projected beam by a larger amount, $\Delta/\tan\alpha$. Therefore, for maximum sensitivity to beam position changes one should select the smallest angle possible. Setting α such that the footprint of the beam illuminates about 75% of the elements provides the optimum sensitivity for beam movements for the given beam size and sufficient room left in order to detect beam displacements.
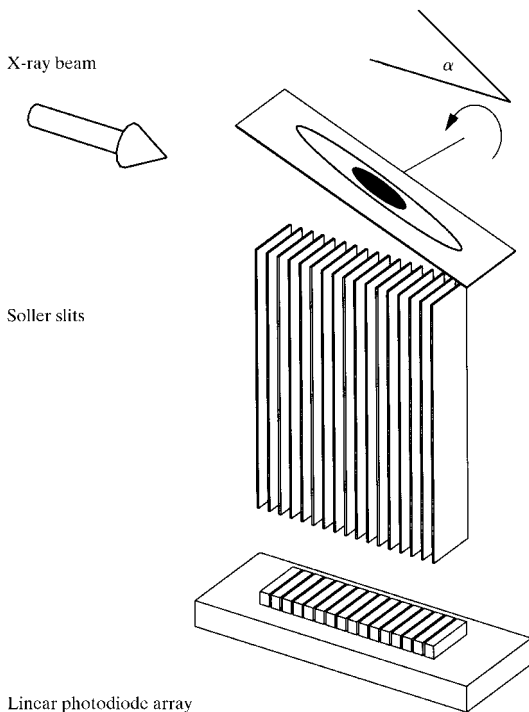
In contrast to conventional beam-intensity monitors the diffusely scattered radiation is measured by a linear array of photodiodes. The solid angle observed by each photodiode element is defined by a Soller slit system mounted directly in front of the diode array. This slit system consists of 21 pieces of 50×10 mm^2 molybdenum foil stacked on top of each other and separated by two 0.75 mm-thick aluminium spacers. The dimensions of the slit openings are 3×0.75 mm^2 and correspond to the size of the individual diode elements. The thickness of the molybdenum foils is 150 µm which matches the distance between the diode elements on the chip. The diode array is shielded from any charged particles and visible light by a thin aluminium foil.

Schottky barrier diodes or standard photodiodes which consist of a simple p–n junction possess an unbiased depletion layer with a typical width of 0.1–1 µm (Sze, 1981) and are therefore less suited for the detection of highly penetrating X-rays. Photodiodes may be fabricated with a thicker depletion layer by inserting an intrinsic or low-doped silicon layer between the p- and n-type material. Such diodes are commonly known as PIN and PNN$^+$
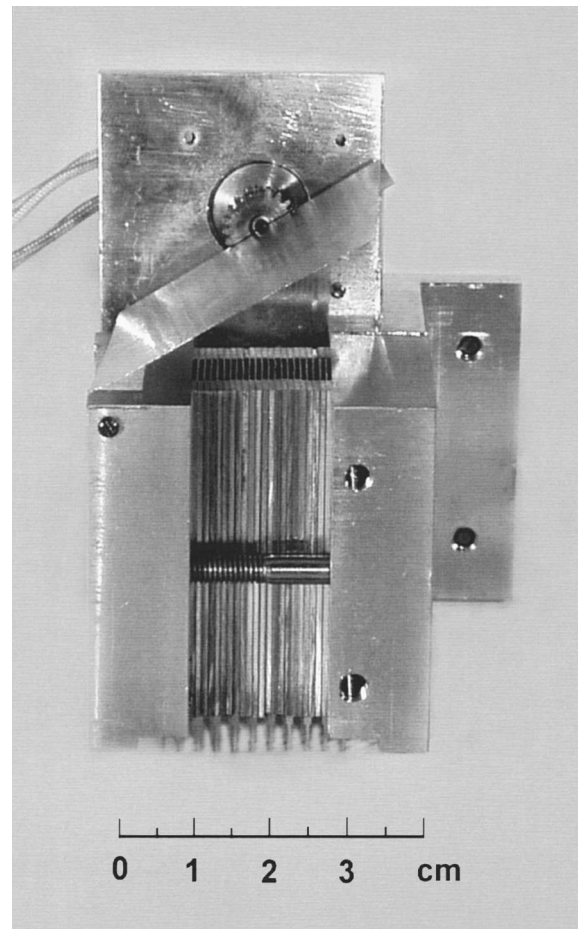

Figure 1
Schematic of the beam monitor. A negligible part of the main X-ray beam is scattered by a thin foil towards a linear diode array. The part of the foil visible to each individual diode element is defined by Soller slits. By changing the angle of the foil with the beam, the footprint of the X-ray can be set for optimum beam-position sensitivity.

Figure 2
Photograph of the test device. The linear diode element is mounted directly below the Soller slit system. At the top of the picture a self-supporting aluminium foil glued to the axis of a stepper motor is clearly visible.

diodes, respectively. The photodiodes in the array that we use for our monitor belong to a class of devices (Korde *et al.*, 1993) with a thick (20–60 µm) low-doped depletion layer. A further two unique features of these diodes are particularly suited for our application. First, the reverted n-on-p structure of the diode with a thin p-doped n-layer has no 'dead' region near the active junction, *i.e.* there is no 'loss' of photogenerated charge carriers due to recombination. Secondly, a special ultrathin (6 nm) nitrided silicon oxide protective top layer makes the photodiodes extremely radiation hard and insensitive to contaminants.

A photograph of our device is shown in Fig. 2. The foil angle α is set by a small vacuum-compatible stepper motor with a step size of 0.8° (Phytron, Germany). The photoelectric signals generated by each diode segment are multiplexed and fed to a current amplifier (Keithley Inc., USA). The voltage output of this transimpedance amplifier is transformed into a 16-bit value by an analog-to-digital (AD) converter. Multiplexer and AD converter are connected to a flexible data-acquisition system based on a network of low-cost commercial modules (Advantech Co. Ltd, Taiwan) that interface to a personal computer through a serial (COM) port.

3. Test results

The performance tests of the beam monitor have been carried out at bending-magnet beamline X12 of the DORIS III positron storage ring using polychromatic radiation. A water-cooled slit system located at a distance of 24 m from the source was used to define the size of the polychromatic test beam. The accuracy with which the individual slit blades are set is estimated to be ±0.02 mm.

The beam monitor was placed on a precision ultrahigh-vacuum-compatible linear drive system and inserted into the beam path about 50 cm downstream of the slit system. The scattering foil was chosen to be a 50 µm-thick carbon foil. A high-precision (±0.2 µm) optical encoder (Heiden-
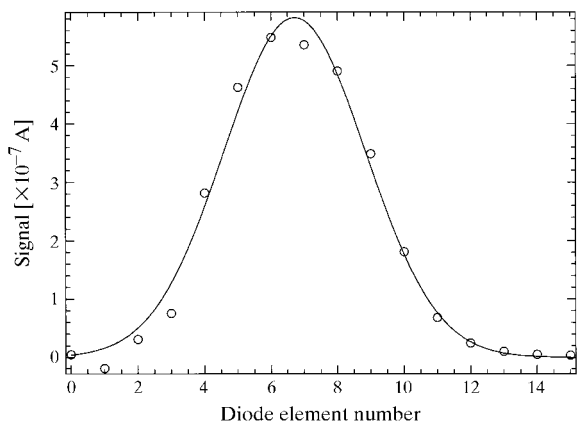
hain, Germany) was used to record the position of the beam monitor. Full control of the device was accomplished by interfacing both translation stage and linear encoder to the aforementioned personal computer. As there were just four digital output lines available to control the multiplexer, we utilized only the inner 16 diode elements using the data-acquisition system.

The response of the device to changes in the beam position were measured by translating the beam monitor through the X-ray beam using the linear drive system. For each position of the monitor the photocurrent generated by the diode elements was measured and the centre of the distribution was determined by a least-squares fit of a Gaussian to the data (see Fig. 3). In the lower panel of Fig. 4 we have plotted the centre of the intensity distribution, as determined by the best-fit result, against the position of the monitor as measured by the optical encoder. The deviation between the best linear fit to the data and the data points, the residue, is shown in the upper panel of Fig. 4. The error bar in the position of the centre, as determined by the fit result, is smaller than the size of the symbols. From the data we conclude that the accuracy by which the beam position changes are measured is better than 1 µm. This value is obtained by dividing the size of the residue by the linear coefficient as determined by the fit. From Fig. 4 one clearly sees that when the intensity distribution is shifted asymmetric to either side of the linear diode array the residue increases and the accuracy by which the centre of the distribution is measured decreases.

To provide an estimate of the true intensity distribution of the projected beam a fitted Gaussian is required to be deconvoluted to remove the effects of instrumental distortion. This distortion is described by the instrumental response function which was determined by performing a measurement with an extremely small footprint of the beam on the foil. This was achieved by reducing the beam
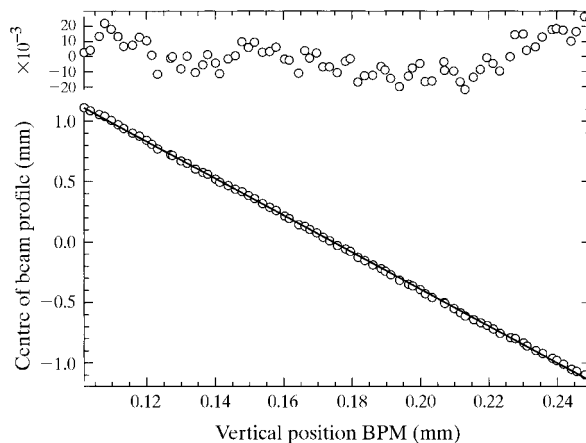
Figure 3
The intensity distribution over the linear diode array as measured with 'white' synchrotron radiation. The solid line is a fit to the data using a single Gaussian curve.

Figure 4
A scan of the beam monitor through a polychromatic X-ray beam. Plotted in the lower panel is the centre of the intensity distribution *versus* the vertical position of the beam-position monitor (BPM) as measured with a high-precision encoder. The top panel shows the best-fit residue.

height and observing the intensity distribution at high angles of incidence, corresponding to the smallest footprint of the beam on the foil (see inset of Fig. 5). It was found that all projected intensity distributions as a function of foil angle are described to a good approximation by a Gaussian (including the limiting case of large incidence angle). Given the widths of the Gaussians fitted to the measured intensity distribution, and the instrumental response function, denoted by δ_m and δ_0, respectively, the (Gaussian) width δ of the true intensity distribution is calculated using the standard formula for the width of the convolution of two Gaussians,

$$\delta_m^2 = \delta^2 + \delta_0^2. \tag{1}$$

In Fig. 5 the true width δ of the measured intensity distribution as a function of the foil angle α for a given beam size is shown. The full drawn line is a fit to the data using

$$\delta = \zeta / \tan(\alpha - \alpha_0), \tag{2}$$

where ζ and α_0 are fitting parameters for beam height and offset angle of the foil, respectively. After the calibration of the foil angle we measured intensity distributions at a fixed foil angle of 7.2° for several values of the beam height. For comparison we also measured the height of the beam using a scan of the foil angle and using (2). The beam height was changed by varying the position of the upper slit blade water-cooled slits in steps of 0.05 mm. The results of these measurements are summarized in Table 1.

The response of the device to a monochromatic beam was investigated by replacing the carbon foil with a 50 μm-thick aluminium foil. An Si(111) channel-cut monochromator was inserted between the slit system and beam monitor. Compared with the experiments with polychromatic radiation the signals were about four orders of magnitude weaker. Nevertheless, we could still perform the same experiments as presented earlier without any difficulty.
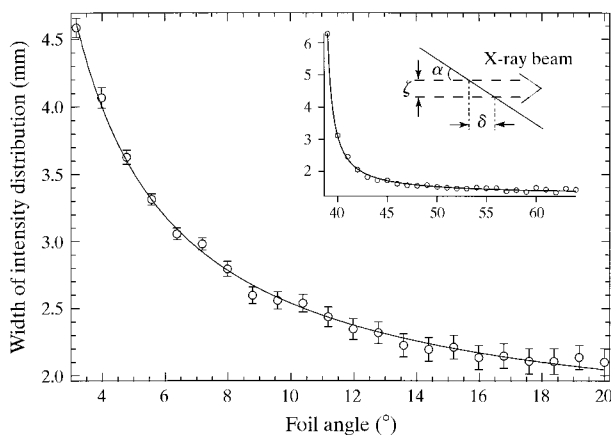
Table 1
Measurements of beam height (mm) with their error bars in parentheses.

The height of the polychromatic beam was set by the water-cooled slit system and its size is given in the left-hand column. In the middle column the beam height ζ as derived from a fit of (2) to the measured width of the intensity distribution as a function of foil angle is listed. The right-hand column lists the height ζ of the beam as derived from the width of the intensity distribution as measured at a fixed foil angle.

	Measured beam height ζ (mm)	
Slit setting (mm)	Foil angle scan	Fixed foil
0.20 (2)	0.24 (1)	0.29 (1)
0.25 (2)	0.26 (1)	0.30 (2)
0.30 (2)	0.29 (2)	0.32 (2)
0.35 (2)	0.31 (2)	0.32 (3)
0.40 (2)	0.33 (2)	0.33 (3)

4. Discussion

The spatially resolved detection of radiation scattered diffusely from a thin foil has been shown to be a useful means of eliciting a comprehensive characterization of an X-ray beam. This technique allows the determination of the total flux (the sum over all diode element signals), the beam position and beam profile. The Gaussian fitting procedure can be performed in a fraction of the time required to re-align the beamline components mechanically. Thus, the additional delay in response due to computation is negligible.

Once an aligned and focused beam has been obtained and characterized by a Gaussian fit, deviations from that optimum condition are indicated by a change in the goodness-of-fit parameter (χ^2). This has proved to be a particularly sensitive method for maintaining beam brightness, even though the resolution of the device for the profile measurement of the beam is limited by the number and size of the diode elements.
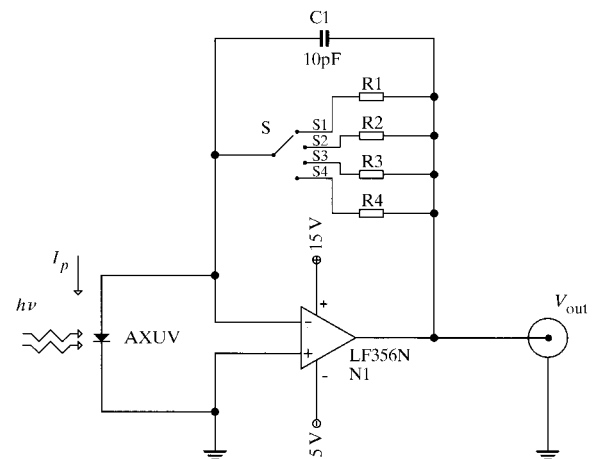

Figure 5
The width of the measured intensity distribution as a function of the angle α of the foil with the X-ray beam. The solid line is a fit to the data according to a simple geometric model of the scattering geometry. The inset shows the calibration scan of foil angle against the width of the intensity distribution expressed in diode elements.

Figure 6
Circuit diagram of the proposed current amplifier. The gain of the device is selected with the indicated switch S. The output voltage V_{out} is given by the product of resistor value Ri ($i = 1, \ldots, 4$) and photocurrent I_p for switch setting Si.

Our design principle is easily extended to a device that measures the beam position and X-ray flux density distribution for both horizontal and vertical directions. Such a device is obtained by a single foil suspended in gimbals, *i.e.* a mount with two mutual orthogonal tilt directions, and a diode matrix or charge coupled device (CCD) detector combined with a crossed Soller slit system to record the diffusely scattered radiation spatially resolved in two dimensions. Standard CCD chips such as used in modern cameras would be a particularly good choice as they combine a high sensitivity with a high resolution (pixel size 7–20 µm).

While the present design is easy to construct, further simplifications could be introduced without impairing its effectiveness. The photocurrents generated by the diodes are sufficiently large to permit the replacement of the current amplifier by inexpensive operational amplifier circuits. In Fig. 6 a circuit diagram of such an amplifier is shown. The amplification of this circuit is determined by the resistor Ri in the feedback loop and allows amplifications up to eight orders of magnitude. Furthermore, the stepper motor that was used to set the angle of incidence with the beam is not strictly necessary. Since the beam height is generally known to a good approximation, a preset angle will suffice in most cases.

Our device is inexpensive and compact, therefore beamline designers would be able to equip beamlines with several devices in order to characterize the beam entering and exiting different optical components. As the devices are suited to permanent monitoring of beam brightness during normal operation, automatic beamline alignment should be possible.

In summary, we have described a versatile beam-position and beam-profile monitor for use with X-ray beamlines. The device is suited to both polychromatic and monochromatic radiation and has none of the disadvantages of existing devices such as cross-term linkage, non-vacuum compatibility or strong wavelength-dependent extinction of the transmitted X-ray beam.

References

Fajardo, P. & Ferrer, S. (1995). *Rev. Sci. Instrum.* **66**, 1879–1881.

Izumi, T., Nakajima, T. & Kurihama, T. (1989). *Rev. Sci. Instrum.* **60**, 1951–1952.

Johnson, E. D. & Oversluizen, T. (1990). *Nucl. Instrum. Methods*, A**291**, 427–430.

Korde, R., Cable, J. S. & Canfield, L. R. (1993). *IEEE Trans. Nucl. Sci.* **40**, 1655–1659.

Koyama, A., Sasaki, S. & Ishikawa, T. (1989). *Rev. Sci. Instrum.* **60**, 1953–1956.

Rosenbaum, G. & Fornek, T. (1997). *AIP Conf. Proc.* **417**, 178.

Silfhout, R. G. van (1998). *Nucl. Instrum. Methods*, A**403**, 153–160.

Sze, S. M. (1981). *Physics of Semiconductor Devices*. New York: John Wiley & Sons.